Distinguishing Competing Mechanistic Manifolds for C(acyl)–N Functionalization by a Ni/*N*-Heterocyclic Carbene Catalyst System

Kaycie R. Malyk‡, Vivek G. Pillai‡, William W. Brennessel, Roberto Leon Baxin, Elliot S. Silk, Daniel T. Nakamura, C. Rose Kennedy*

University of Rochester, Department of Chemistry, Rochester, NY 14627, United States

Supporting Information Placeholder

ABSTRACT: Carboxylic acid derivatives are appealing alternatives to organohalides as cross-coupling electrophiles for fine chemical synthesis due to their prevalence in biomass and bioactive small molecules as well as their ease of preparation and handling. Within this family, carboxamides comprise a versatile electrophile class for nickel-catalyzed coupling with carbon and heteroatom nucleophiles. However, even state-of-the-art C(acyl)–N functionalization and cross-coupling reactions typically require high catalyst loadings and specific substitution patterns. These challenges have proven difficult to overcome, in large part due to limited experimental mechanistic insight. In this work, we describe a detailed mechanistic case study of acylative coupling reactions catalyzed by the commonly employed Ni/SIPr catalyst system (SIPr = 1,3-Bis(2,6-di-isopropylphenyl)-4,5-dihydroimidazol-2-ylidine). Stoichiometric organometallic studies, in situ spectroscopic measurements, and crossover experiments demonstrate accessibility of Ni(0), Ni(I), and Ni(II) resting states. Although in situ precatalyst activation limits reaction efficiency, the low concentrations of active, SIPr-supported Ni(0) select for electrophile-first (closed-shell) over competing nucleophile-first (open-shell) mechanistic manifolds. We anticipate that the experimental insights into the nature and controlling features of these distinct pathways are likely to accelerate rational improvements to cross-coupling methodologies involving pervasive carboxamide substrate motifs.

Over the past decade, tremendous progress has been reported in the use of carboxylic acid derivatives, such as carboxamides, as substrates for catalytic cross coupling.[1-3] Carboxamides are attractive alternatives to traditional organohalide electrophiles due to their relative abundance in biomass and drug-like molecules, ease of synthesis, and avoidance of halogenated waste streams.[4-8] Typically, carboxamide C(acyl)–N functionalization methods rely on Ni catalysis due to the enhanced electropositivity of Ni (which facilitates activation of more polar C–O and C–N bonds) compared to conventional Pd cross-coupling catalysts (which favor reactions with more covalent C–halogen bonds).[9, 10] However, Ni readily undergoes both $1e^-$ and $2e^-$ processes, complicating method development and study. [9, 10 11]

In contrast to conventional Pd-catalyzed cross-coupling reactions,[12-16] the sequence of steps, identities of catalytically active species, and selectivity-determining factors remain ambiguous for Ni-catalyzed coupling reactions with carboxamide electrophiles. Studies of Ni/bisphosphine catalyst systems have begun to shed light on related coupling reactions with carboxylate ester and acyl fluoride electrophiles.[17-19] However, complementary Ni/ *N*-heterocyclic carbene (NHC) catalyst systems remain comparatively understudied. [20-28] This deficiency is noteworthy given the broad variety of acylative coupling reactions that rely on Ni/NHC precatalysts.[22, 29-42] Experimental characterization of catalytically relevant species and steps is thus essential to enable future rational improvements.

Herein, we report the systematic examination of C(acyl)–N functionalization reactions of carboxamide electrophiles catalyzed by the commonly employed combination of Ni and SIPr (SIPr = 1,3-bis(2,6-di-i-propylphenyl)-4,5-dihydroimidazol-2-ylidine). We provide evidence for the accessibility and chemical competence of Ni(0), Ni(I), and Ni(II) resting states in such reactions, where the nucleophile identity and concentrations of C–N activated complexes play key roles in gating access to distinct, off-cycle Ni(I) species. These findings shed light on the baseis for catalyst inefficiencies and limited substrate compatibility, thereby providing the insights needed for rational development of next-generation methodologies with carboxamides and other carboxylic acid-derived electrophiles.

Scheme 1. Model reactions selected for evaluation of competing mechanistic hypotheses. [a]

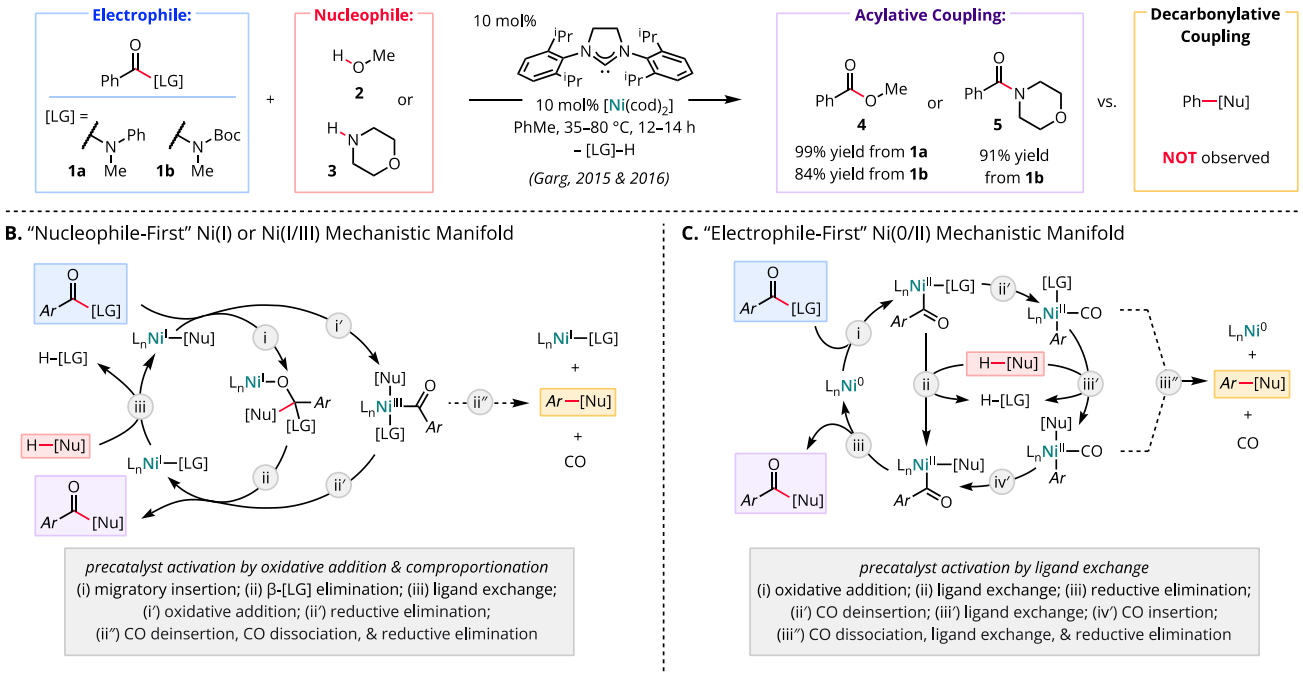

[a] *Ar* = aryl; cod = 1,5-cyclooctadiene; [LG] = leaving group; [Nu] = nucleophile

To probe the pathways involved in Ni-catalyzed C(acyl)–N functionalization, we elected to examine the landmark catalytic esterification and transamidation methodologies reported by Garg and coworkers in 2015 and 2016 (Scheme 1A).[22,29] These catalytic methods achieve carbonyl-retentive C–heteroatom bond-formation between alcohol or amine nucleophiles and *N*-functionalized benzamide electrophiles, which are commonly described as twisted amides.[43-45] Although these methods are formally the equivalent of traditional acyl substitution chemistry, they proceed under comparatively mild conditions (room temperature to 80 °C) in the absence of strong Lewis or Brønsted acids. Although many cross-coupling reactions with C(acyl)–N electrophiles require highly twisted amide substrates, which exhibit enhanced electrophilicity due to disrupted n(N) → π*(CO) conjugation,[43,46-49] the heteroatom coupling methods under study notably require only moderately activated substrates.

At the outset of our investigation, we identified two general mechanistic manifolds that could account for the observed, carbonyl-retentive coupling. In a "nucleophile-first" manifold (Scheme 1B), initial formation of a Ni(I) nucleophile adduct would be followed by (i) migratory insertion with the twisted amide electrophile, (ii) β-elimination, and (iii) exchange of the leaving group for nucleophile to turn over the catalytic cycle. A variation of the "nucleophile-first" manifold could alternatively involve (i′) oxidative addition and (ii′) reductive elimination through a Ni (I/III) cycle intercepting many of the same intermediates as the redox-neutral case above.

In an alternative "electrophile-first" manifold (Scheme 1C) (i) initial C–N oxidative addition by Ni(0) would be followed by (ii) ligand exchange and (iii) carbon–nucleophile bond-forming reductive elimination. Despite the surprising preference for carbonyl-retentive reactivity (in contrast to the decarbonylative reactivity often noted with Ni(II) acyl complexes),[17-19] the electrophile-first manifold is generally invoked, with computational studies supporting its energetic feasibility.[21,22] However, no conclusive experimental validation has been disclosed, and to the best of our knowledge, no head-to-head comparison with alternative mechanistic hypotheses (such as the nucleophile-first case) has been conducted. Notably, kinetics alone cannot distinguish between the two manifolds, which may feature rate laws with analogous forms depending on the rate-determining step.[27] Differentiating these pathways instead requires direct identification of catalytically active intermediates.

In light of these mechanistic ambiguities, we first set out to identify the composition/speciation and resting state(s) of nickel under catalytically relevant conditions. In analogy to in situ activation protocols, equimolar [Ni(cod)$_2$] and SIPr were mixed in benzene-d_6 (0.1 M) at room temperature (approx. 22 °C) and monitored by ^{1}H NMR spectroscopy (Scheme 2A). Generation of [(SIPr)Ni(C_6D_6)] (**6**) was noted, but even after mixing for several hours, substantial [Ni(cod)$_2$] and SIPr remained in solution ([SIPr]:**6** = [Ni(cod)$_2$]:[cod]/2 = 2:1). Although [Ni(SIPr)$_2$] has previously been suggested as the primary catalyst resting state,[22] it was not detected when employing a 1:1 ratio of [Ni] and ligand. Under catalytic conditions (10 mol% [Ni(cod)$_2$]; 10 mol% SIPr) in the presence of amide **1a** and methanol (**2**), the low concentrations of **6** generated in situ were depleted but substantial [Ni(cod)$_2$] and SIPr remained even after several hours, comprising an off-cycle catalyst resting state (Scheme 2B). In control experiments, neither [Ni(cod)]$_2$ nor SIPr alone catalyzed the acylative couplings under investigation. As such, these findings are

consistent with inefficient formation of **6** or another active catalyst necessitating the relatively high loadings (≥10 mol%) typically required for these transformations.

To better assess the identities and catalytic competencies of the nickel-containing species generated in situ, we deemed it essential to work directly with single-component precatalysts. Following modification of conditions reported previously, the combination of [Ni(cod)$_2$], SIPr•HCl, and KO^{t}Bu in benzene under H_2 pressure (~1 atm, to effect the hydrogenation of 1,5-cyclooctadiene) afforded direct access to **6** (Scheme 2A).[50]

Scheme 2. In Situ Precatalyst Activation is Inefficient.[a]

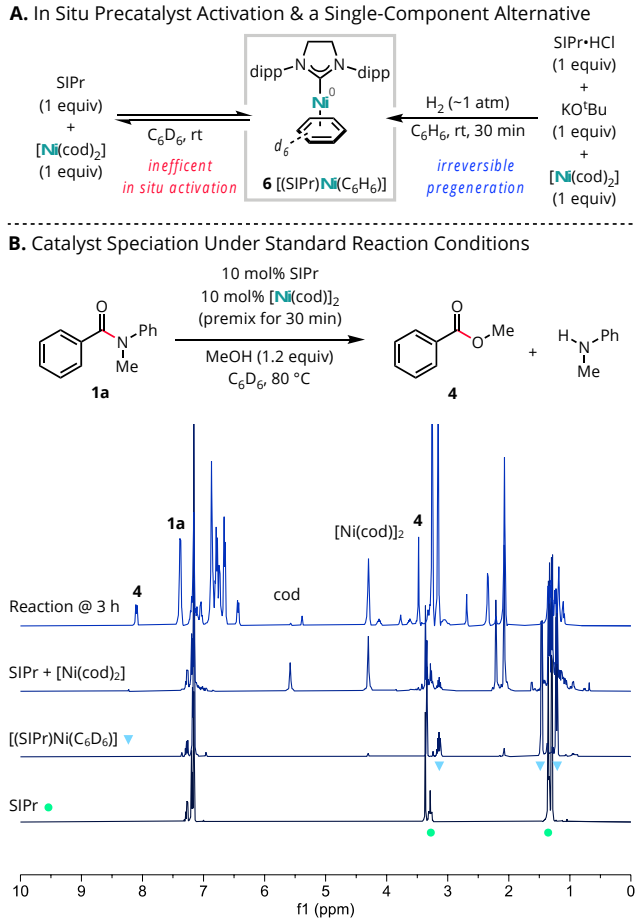

[a] dipp = 2,6-diisopropylphenyl; cod = 1,5-cyclooctadiene

Hartwig and coworkers demonstrated previously that treating **6** with phenol resulted in the formation of nickel(I) phenoxide dimer [(SIPr)Ni(OPh)]$_2$ (**7a**) via sequential oxidative addition comproportionation (Scheme 3A).[51-53] Although phenols are poor substrates for the nickel-catalyzed esterification, presumably due to the low thermodynamic driving force for formation of the corresponding phenyl esters, we postulated that **7a** could act as a shunt into the nucleophile-first mechanistic manifold through ligand exchange to access on-cycle Ni(I) nucleophile adducts. Consistent with this hypothesis, using **7a** (5 mol% dimer, 10 mol% [Ni]) in place of SIPr/[Ni(cod)$_2$] under otherwise standard conditions resulted in formation of ester **4** (9% yield), albeit with reduced conversion relative to standard conditions (Scheme 3B).

We thus sought to determine whether the alcohol and amine nucleophiles applied for the model reactions could, in analogy to phenol, promote access to nickel(I).[54,55] Mixing **6** with **2** or **3** (2.0 equiv) in benzene-d_6 at room temperature up to 80 °C afforded negligible reactivity with no new species detected by ^{1}H NMR until eventual decomposition of [(SIPr)Ni(C$_6$D$_6$)] (Scheme 3A).[56,57] Taken together, these results suggest that oxidative addition into the stronger, less acidic O–H/N–H bonds of unactivated alcohols or amines is negligible in catalytically relevant arene solvents. However, these findings did not rule out the possibility of accessing Ni(I) species from alternative Ni(II) sources generated in situ (see below).

Scheme 3. Access to and Viability of Catalytically Relevant Nickel(I) Complexes.

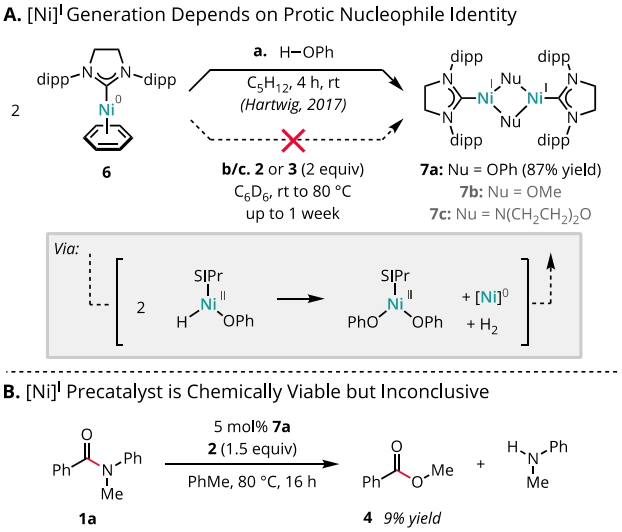

We next assessed the reactivity of single-component Ni(0) precatalyst **6** toward representative twisted amide substrates across a range of amidicities (Scheme 4A).[44,48,58] Amides **1b–d** underwent clean conversion to the corresponding SIPr-supported Ni(II) acyl products, which were isolated in 43–81% yield and characterized by SC-XRD (Figure 1), confirming their composition and connectivity. Although no oxidative addition products were detected with substrates lacking a carbamate directing group (e.g. **1a**), a crossover experiment between **1a** and fluorine-tagged substrate **1e** provided support for their kinetic accessibility (Scheme 4B).[59-61]

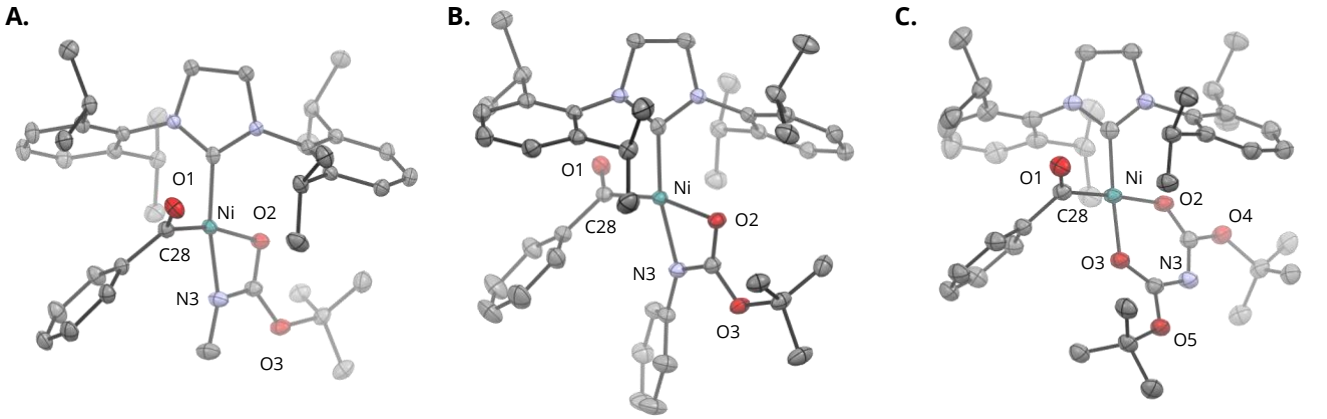

Figure 1. Solid-state structures of (A.) **8b** (B.) **8c**, and (C.) **8d** determined by SC-XRD. Thermal ellipsoids depicted at 50% probability. H-atoms and co-crystallized solvent molecules omitted for clarity. C = charcoal, N = blue, O = red, Ni = teal

The solid-state structures for **8b–d** determined by SC-XRD (Figure 1) exhibited chelation by the carbamate directing group in either a κ^2-N,O or κ^2-O,O arrangement, resulting in distorted square planar coordination geometries (**8b**: $\tau_4 = 0.17$; **8c**: $\tau_4 = 0.19$; **8d**: $\tau_4 = 0.10$).[62] In both complexes **8b** and **8c**, the NHC was found mutually *cis* to the benzoyl group, *cis* to the carbamate O, and *trans* to N in an arrangement minimizing steric interference with the bulking ligand wingtip substituents. While the geometric parameters for **8b** and **8c** were near-identical, complex **8d**, demonstrated a 6-membered chelate with the two carbamate directing groups. Although such chelates have been described for phosphine-based catalyst systems,[63] computational studies of NHC-based catalyst systems have instead invoked 3-centered oxidative addition with disagreement over the role of directing-group assistance or chelation post-oxidative addition.[21,28]

We next evaluated the chemical and catalytic competencies of these well-defined Ni(II) acyl complexes for the acylative coupling model reactions. Even at room temperature, complexes **8b** and **8c** react with excess nucleophile in benzene-d_6 to yield acyl coupling products **4** (37% yield from **8b**) and **5** (30% yield from **8b**) within 24 hours. Reformation of **6** was observed, but no other organometallic intermediates were detected under these conditions. Using **8c** (10 mol%) in place of [Ni(cod)$_2$]/SIPr under otherwise standard conditions similarly resulted in clean formation of product **4** (90% yield).

Scheme 4. Kinetic Accessibility and Catalytic Relevance of C(acyl)–N Oxidative Addition

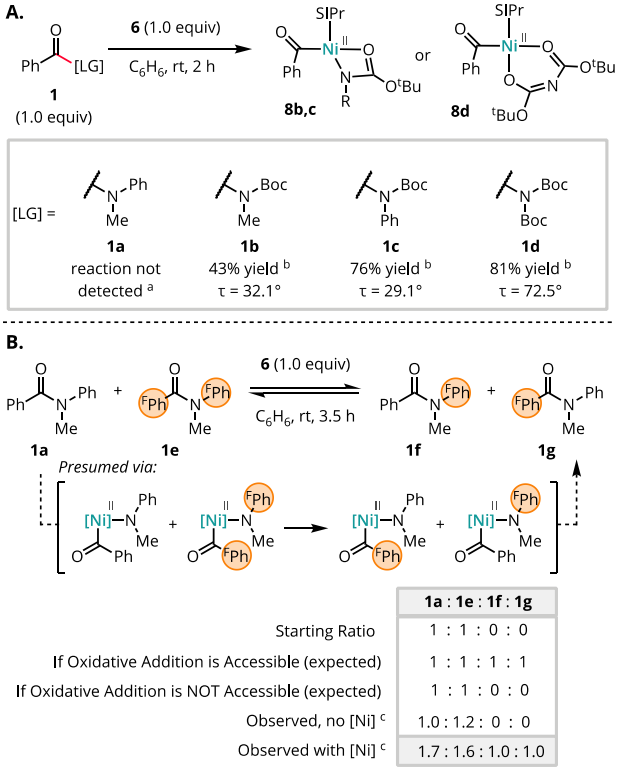

a Up to 80 °C. b Isolated yields validated by integration of diagnostic ^{1}H NMR resonances relative to 1,3,5-trimethoxybenzene as an internal standard. Winkler–Dunitz Distortion twist angles (τ) from Ref 44–46. c Relative integration of diagnostic signals detected by analytical gas chromatography.

The chemical and catalytic competence of the Ni(II) acyl species supports the viability of the electrophile-first mechanistic manifold. However, an alternative providing access to Ni(I) and the nucleophile-first mechanistic manifold could not be excluded. In this case, reversible reductive elimination from the Ni(II) acyl species would enable Ni(0)–Ni(II) comproportionation. To evaluate the

feasibility of this latter possibility, we examined the reactivity between **6** and Ni(II) acyl complex **8c** in C_6H_6 at 80 °C (Scheme 5). The ^1H NMR spectrum obtained after 5 hours revealed complete consumption of both Ni complexes and the formation of at least two new species, including major components with paramagnetically-shifted resonances. Further characterization of the resulting species by X-band electron paramagnetic resonance (EPR) spectroscopy in THF glass at 10 K afforded two sets of rhombic signals (simulated as g_A = [2.92, 2.38, 2.01], g_B = [2.54, 2.37, 2.01]). However, deploying this mixture of species as the precatalyst under otherwise standard conditions promoted reactivity with inverted chemoselectivity. Instead of ester **4**, products **9** and **10** resulting from attack of the carbamoyl activating group were formed. In light of these findings, we hypothesize that the inefficient in situ precatalyst activation limits the concentrations of SIPr-supported Ni(0) and Ni(II), thereby inhibiting counterproductive Ni(I) generation.

Scheme 5. Evidence for Comproportionation of Amide Oxidative Addition Products.

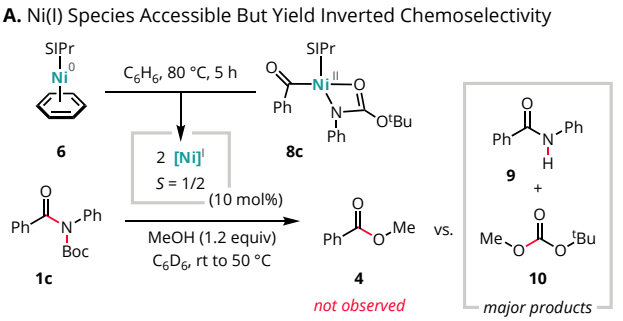

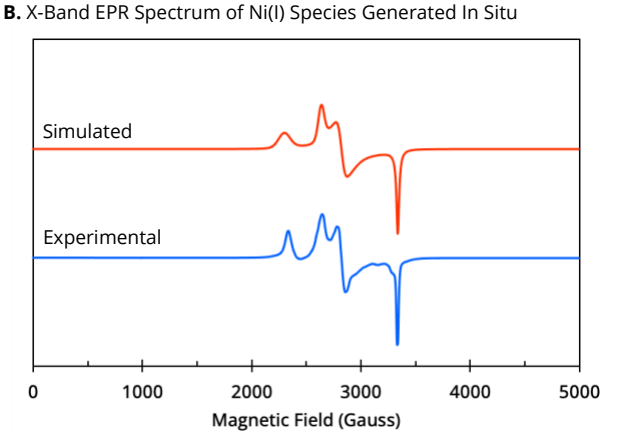

Taken together, these stoichiometric organometallic studies, in situ spectroscopic measurements, and crossover experiments provide evidence for the accessibility of Ni(0), Ni(II), *and* Ni(I) complexes under catalytically relevant conditions. Our work provides the first unambiguous experimental validation of the presumptive electrophile-first mechanistic manifold but also supports the viability of a competing nucleophile-first mechanistic manifolds that induce counterproductive chemoselectivity. We anticipate that these findings will provide a nuanced understanding of coupling reactions to enable new and more efficient coupling reactions involving abundant acyl electrophiles.

ASSOCIATED CONTENT

Supporting Information

The Supporting Information is available free of charge on the ACS Publications website.

Experimental details, compound characterization data, computational methods, and results (PDF)

Crystallographic data for **8b** (CCDC 2264311), **8c** (CCDC 2264313), and **8d** (CCDC 2264312)(CIF)

AUTHOR INFORMATION

Corresponding Author

C. Rose Kennedy — Department of Chemistry, University of Rochester, Rochester, New York 14627; orcid.org/0000-0003-3681-819X Email: c.r.kennedy@rochester.edu

Authors

Kaycie Malyk — Department of Chemistry, University of Rochester, Rochester, New York 14627; orcid.org/0000-0002-7515-0658

Vivek G. Pillai — Department of Chemistry, University of Rochester, Rochester, New York 14627; orcid.org/0009-0004-8918-5597

William W. Brennessel — Department of Chemistry, University of Rochester, Rochester, New York 14627; orcid.org/0000-0001-5461-1825

Roberto Leon Baxin — Department of Chemistry, University of Rochester, Rochester, New York 14627; orcid.org/0009-0004-5410-6051

Elliot S. Silk — Department of Chemistry, University of Rochester, Rochester, New York 14627; orcid.org/0000-0001-9592-7631

Daniel T. Nakamura — Department of Chemistry, University of Rochester, Rochester, New York 14627; orcid.org 0000-0003-1288-0271

Author Contributions

† Authors K. R. M. and V. G. P. contributed equally. Although listed order is alphabetical by last name, both are entitled to list their own name first on publication lists.

Notes

The authors declare no competing financial interest.

ACKNOWLEDGMENT

Financial support was provided by the University of Rochester and David and Lucille Packard Foundation (#2022-74673). E.S.S. acknowledges the University of Rochester Discover Grant for a research fellowship. The NSF MRI program is acknowledged for the purchase of an X-ray diffractometer (CHE-1725028). The authors thank Dr.s Jason Holt and Tessa Baker (University of Rochester) for instrumentation assistance and Jorge A. Castaños Valencia (Universidad del Valle) for synthetic assistance. The authors thank Dr.s William Jones (University of Rochester), Shauna Paradine (University of Rochester), and Joseph Gair (Michigan State University) for insightful comments and critiques.

REFERENCES

1. Dander, J. E.; Garg, N. K. Breaking Amides using Nickel Catalysis. *ACS Catal.* **2017**, *7*, 1413–1423. DOI: 10.1021/acscatal.6b03277
2. Takise, R.; Muto, K.; Yamaguchi, J. Cross-coupling of aromatic esters and amides. *Chem. Soc. Rev.* **2017**, *46*, 5864–5888. DOI: 10.1039/C7CS00182G
3. Boit, T. B.; Bulger, A. S.; Dander, J. E.; Garg, N. K. Activation of C–O and C–N Bonds Using Non-Precious-Metal Catalysis. *ACS Catal.* **2020**, *10*, 12109–12126. DOI: 10.1021/acscatal.0c03334
4. For example, carboxamides are found in over 50% of small-molecule pharmaceuticals, and amidation is the most common reaction class employed in medicinal chemistry settings. See ref. 5–8.
5. Walters, W. P.; Green, J.; Weiss, J. R.; Murcko, M. A. What Do Medicinal Chemists Actually Make? A 50-Year Retrospective. *J. Med. Chem.* **2011**, *54*, 6405–6416. DOI: 10.1021/jm200504p
6. Roughley, S. D.; Jordan, A. M. The Medicinal Chemist's Toolbox: An Analysis of Reactions Used in the Pursuit of Drug Candidates. *J. Med. Chem.* **2011**, *54*, 3451–3479. DOI: 10.1021/jm200187y
7. Ertl, P.; Altmann, E.; McKenna, J. M. The Most Common Functional Groups in Bioactive Molecules and How Their Popularity Has Evolved over Time. *J. Med. Chem.* **2020**, *63*, 8408–8418. DOI: 10.1021/acs.jmedchem.0c00754
8. Bhutani, P.; Joshi, G.; Raja, N.; Bachhav, N.; Rajanna, P. K.; Bhutani, H.; Paul, A. T.; Kumar, R. U.S. FDA Approved Drugs from 2015–June 2020: A Perspective. *J. Med. Chem.* **2021**, *64*, 2339–2381. DOI: 10.1021/acs.jmedchem.0c01786
9. Tasker, S. Z.; Standley, E. A.; Jamison, T. F. Recent advances in homogeneous nickel catalysis. *Nature* **2014**, *509*, 299-309. DOI: 10.1038/nature13274
10. Diccianni, J. B.; Diao, T. N. Mechanisms of Nickel-Catalyzed Cross-Coupling Reactions. *Trends Chem* **2019**, *1*, 830–844. DOI: 10.1016/j.trechm.2019.08.004
11. The redox versatility also introduces opportunities for innovation and an parallel area of vibrant research takes advantage of the unique 1-electron chemistry at nickel.
12. Thomas, A. A.; Denmark, S. E. Pre-transmetalation intermediates in the Suzuki-Miyaura reaction revealed: The missing link. *Science* **2016**, *352*, 329-332. DOI: 10.1126/science.aad6981
13. Thomas, A. A.; Wang, H.; Zahrt, A. F.; Denmark, S. E. Structural, Kinetic, and Computational Characterization of the Elusive Arylpalladium(II)boronate Complexes in the Suzuki–Miyaura Reaction. *J. Am. Chem. Soc.* **2017**, *139*, 3805–3821. DOI: 10.1021/jacs.6b13384
14. Hartwig, J. F. Electronic Effects on Reductive Elimination To Form Carbon–Carbon and Carbon–Heteroatom Bonds from Palladium(II) Complexes. *Inorg. Chem.* **2007**, *46*, 1936–1947. DOI: 10.1021/ic061926w
15. Hartwig, J. F.; Collman, J. P. *Organotransition metal chemistry: from bonding to catalysis*. University Science Books Sausalito, CA: 2010; Vol. 1.
16. D'Alterio, M. C.; Casals-Cruañas, È.; Tzouras, N. V.; Talarico, G.; Nolan, S. P.; Poater, A. Mechanistic Aspects of the Palladium-Catalyzed Suzuki-Miyaura Cross-Coupling Reaction. *Chem. Eur. J.* **2021**, *27*, 13481–13493. DOI: 10.1002/chem.202101880
17. Lalloo, N.; Brigham, C. E.; Sanford, M. S. Mechanism-Driven Development of Group 10 Metal-Catalyzed Decarbonylative Coupling Reactions. *Acc. Chem. Res.* **2022**, *55*, 3430–3444. DOI: 10.1021/acs.accounts.2c00496
18. Guo, L.; Rueping, M. Decarbonylative Cross-Couplings: Nickel Catalyzed Functional Group Interconversion Strategies for the Construction of Complex Organic Molecules. *Acc. Chem. Res.* **2018**, *51*, 1185–1195. DOI: 10.1021/acs.accounts.8b00023
19. Guo, L.; Rueping, M. Transition-Metal-Catalyzed Decarbonylative Coupling Reactions: Concepts, Classifications, and Applications. *Chem. Eur. J.* **2018**, *24*, 7794–7809. DOI: 10.1002/chem.201704670
20. Although several computational studies have been reported (Ref 21–25), experimental validation has been much more limited (Ref 26–28).
21. Wang, H.; Zhang, S.-Q.; Hong, X. Computational studies on Ni-catalyzed amide C–N bond activation. *Chem. Commun.* **2019**, *55*, 11330–11341. DOI: 10.1039/C9CC05763C
22. Hie, L.; Nathel, N. F. F.; Shah, T. K.; Baker, E. L.; Hong, X.; Yang, Y. F.; Liu, P.; Houk, K. N.; Garg, N. K. Conversion of amides to esters by the nickel-catalysed activation of amide C-N bonds. *Nature* **2015**, *524*, 79–83. DOI: 10.1038/nature14615
23. Liu, L. L.; Chen, P.; Sun, Y.; Wu, Y.; Chen, S.; Zhu, J.; Zhao, Y. Mechanism of Nickel-Catalyzed Selective C–N Bond Activation in Suzuki-Miyaura Cross-Coupling of Amides: A Theoretical Investigation. *J. Org. Chem.* **2016**, *81*, 11686–11696. DOI: 10.1021/acs.joc.6b02093
24. Xu, Z.-Y.; Yu, H.-Z.; Fu, Y. Mechanism of Nickel-Catalyzed Suzuki–Miyaura Coupling of Amides. *Chem. Asian J.* **2017**, *12*, 1765-1772. DOI: 10.1002/asia.201700313
25. Chu, C.-q.; Dang, L. Esterification of Aryl and Alkyl Amides Enabled by Tailor-Made and Proposed Nickel Catalyst: Insights from Theoretical Investigation. *J. Org. Chem.* **2018**, *83*, 5009–5018. DOI: 10.1021/acs.joc.8b00160
26. Hu, J.; Zhao, Y.; Liu, J.; Zhang, Y.; Shi, Z. Nickel-Catalyzed Decarbonylative Borylation of Amides: Evidence for Acyl C–N Bond Activation. *Angew. Chem. Int. Ed.* **2016**, *55*, 8718-8722. DOI: 10.1002/anie.201603068
27. Weires, N. A.; Caspi, D. D.; Garg, N. K. Kinetic Modeling of the Nickel-Catalyzed Esterification of Amides. *ACS Catal.* **2017**, *7*, 4381-4385. DOI: 10.1021/acscatal.7b01444 (doi: 10.1021/acscatal.7b01444)
28. Zhong, H.; Egger, D.; Gasser, V.; Finkelstein, P.; Keim, L.; Seidel, M.; Trapp, N.; Morandi, B. Skeletal Metalation of Lactams through Carbonyl-to-Nickel Exchange Logic. *ChemRxiv* **2023**. DOI: 10.26434/chemrxiv-2023-4mw5f
29. Baker, E. L.; Yamano, M. M.; Zhou, Y. J.; Anthony, S. M.; Garg, N. K. A two-step approach to achieve secondary amide transamidation enabled by nickel catalysis. *Nat. Commun.* **2016**, *7*, 11554. DOI: 10.1038/ncomms11554
30. Hie, L.; Baker, E. L.; Anthony, S. M.; Desrosiers, J. N.; Senanayake, C.; Garg, N. K. Nickel-Catalyzed Esterification of Aliphatic Amides. *Angew. Chem. Int. Ed.* **2016**, *55*, 15129–15132. DOI: 10.1002/anie.201607856
31. Simmons, B. J.; Weires, N. A.; Dander, J. E.; Garg, N. K. Nickel-Catalyzed Alkylation of Amide Derivatives. *ACS Catal.* **2016**, *6*, 3176–3179. DOI: 10.1021/acscatal.6b00793
32. Weires, N. A.; Baker, E. L.; Garg, N. K. Nickel-catalysed Suzuki-Miyaura coupling of amides. *Nat. Chem.* **2016**, *8*, 75–79. DOI: 10.1038/NCHEM.2388
33. Ito, Y.; Nakatani, S.; Shiraki, R.; Kodama, T.; Tobisu, M. Nickel-Catalyzed Addition of C–C Bonds of Amides to Strained Alkenes: The 1,2-Carboaminocarbonylation Reaction. *J. Am. Chem. Soc.* **2022**, *144*, 662–666. DOI: 10.1021/jacs.1c09265
34. Zheng, Y.-L.; Xie, P.-P.; Daneshfar, O.; Houk, K. N.; Hong, X.; Newman, S. G. Direct Synthesis of Ketones from Methyl Esters by Nickel-Catalyzed Suzuki–Miyaura Coupling. *Angew. Chem. Int. Ed.* **2021**, *60*, 13476–13483. DOI: 10.1002/anie.202103327
35. Ben Halima, T.; Masson-Makdissi, J.; Newman, S. G. Nickel-Catalyzed Amide Bond Formation from Methyl Esters. *Angew. Chem. Int. Ed.* **2018**, *57*, 12925–12929. DOI: 10.1002/anie.201808560
36. Zheng, Y.-L.; Newman, S. G. Methyl Esters as Cross-Coupling Electrophiles: Direct Synthesis of Amide Bonds. *ACS Catal.* **2019**, *9*, 4426–4433. DOI: 10.1021/acscatal.9b00884
37. Zheng, Y.-L.; Newman, S. G. Nickel-Catalyzed Domino Heck-Type Reactions Using Methyl Esters as Cross-Coupling Electrophiles. *Angew. Chem. Int. Ed.* **2019**, *58*, 18159–18164. DOI: 10.1002/anie.201911372

38. Walker, J. A.; Vickerman, K. L.; Humke, J. N.; Stanley, L. M. Ni-Catalyzed Alkene Carboacylation via Amide C-N Bond Activation. *J. Am. Chem. Soc.* **2017**, *139*, 10228–10231. DOI: 10.1021/jacs.7b06191
39. Li, J.-F.; Wang, Y.-F.; Wu, Y.-Y.; Liu, W.-J.; Wang, J.-W. Nickel-Catalyzed Esterification of Amides Under Mild Conditions. *Catal. Lett.* **2020**, *150*, 874–880. DOI: 10.1007/s10562-019-02966-6
40. Buchspies, J.; Rahman, M. M.; Szostak, M. Suzuki–Miyaura Cross-Coupling of Amides Using Well-Defined, Air- and Moisture-Stable Nickel/NHC (NHC = N-Heterocyclic Carbene) Complexes. *Catalysts* **2020**, *10*, 372. DOI: 10.3390/catal10040372
41. Buchspies, J.; Szostak, M. Recent Advances in Acyl Suzuki Cross-Coupling. *Catalysts* **2019**, *9*, 53.
42. Li, G.; Szostak, M. Non-Classical Amide Bond Formation: Transamidation and Amidation of Activated Amides and Esters by Selective N–C/O–C Cleavage. *Synthesis* **2020**, *52*, 2579-2599. DOI: 10.1055/s-0040-1707101
43. Liu, C. W.; Szostak, M. Twisted Amides: From Obscurity to Broadly Useful Transition-Metal-Catalyzed Reactions by N-C Amide Bond Activation. *Chem. Eur. J.* **2017**, *23*, 7157–7173. DOI: 10.1002/chem.201605012
44. Meng, G.; Zhang, J.; Szostak, M. Acyclic Twisted Amides. *Chem. Rev.* **2021**, *121*, 12746–12783. DOI: 10.1021/acs.chemrev.1c00225
45. Gao, P.; Rahman, M. M.; Zamalloa, A.; Feliciano, J.; Szostak, M. Classes of Amides that Undergo Selective N–C Amide Bond Activation: The Emergence of Ground-State Destabilization. *J. Org. Chem.* **2022**. DOI: 10.1021/acs.joc.2c01094
46. Szostak, R.; Shi, S. C.; Meng, G. R.; Lalancette, R.; Szostak, M. Ground-State Distortion in N-Acyl-tert-butyl-carbamates (Boc) and N-Acyl-tosylamides (Ts): Twisted Amides of Relevance to Amide N-C Cross-Coupling. *J. Org. Chem.* **2016**, *81*, 8091–8094. DOI: 10.1021/acs.joc.6b01560
47. Szostak, R.; Meng, G.; Szostak, M. Resonance Destabilization in N-Acylanilines (Anilides): Electronically-Activated Planar Amides of Relevance in N–C(O) Cross-Coupling. *J. Org. Chem.* **2017**, *82*, 6373–6378. DOI: 10.1021/acs.joc.7b00971
48. Meng, G. R.; Shi, S. C.; Lalancette, R.; Szostak, R.; Szostak, M. Reversible Twisting of Primary Amides via Ground State N-C(O) Destabilization: Highly Twisted Rotationally Inverted Acyclic Amides. *J. Am. Chem. Soc.* **2018**, *140*, 727–734. DOI: 10.1021/jacs.7b11309
49. The extent of activation or twisting is typically quantified using the Winkler–Dunitz Distortion Parameters including twist angle (τ) about the amide bond and nitrogen pyramidalization parameter (χ). See ref 33.
50. Hoshimoto, Y.; Hayashi, Y.; Suzuki, H.; Ohashi, M.; Ogoshi, S. One-Pot, Single-Step, and Gram-Scale Synthesis of Mononuclear [(η^6-arene)Ni(N-heterocyclic carbene)] Complexes: Useful Precursors of the Ni0–NHC Unit. *Organometallics* **2014**, *33*, 1276-1282. DOI: 10.1021/om500088p
51. Saper, N. I.; Hartwig, J. F. Mechanistic Investigations of the Hydrogenolysis of Diaryl Ethers Catalyzed by Nickel Complexes of N-Heterocyclic Carbene Ligands. *J. Am. Chem. Soc.* **2017**, *139*, 17667–17676. DOI: 10.1021/jacs.7b10537
52. Bismuto, A.; Müller, P.; Finkelstein, P.; Trapp, N.; Jeschke, G.; Morandi, B. One to Find Them All: A General Route to Ni(I)–Phenolate Species. *J. Am. Chem. Soc.* **2021**, *143*, 10642–10648. DOI: 10.1021/jacs.1c03763
53. Lin, C.-Y.; Power, P. P. Complexes of Ni(I): a "rare" oxidation state of growing importance. *Chem. Soc. Rev.* **2017**, *46*, 5347–5399. DOI: 10.1039/C7CS00216E
54. Dodd, N. A.; Bacsa, J.; Sadighi, J. P. Synthesis of a Nickel(I) alkoxide and related cation equivalents. *Polyhedron* **2021**, *208*, 115408. DOI: 10.1016/j.poly.2021.115408
55. Lipschutz, M. I.; Tilley, T. D. Useful Method for the Preparation of Low-Coordinate Nickel(I) Complexes via Transformations of the Ni(I) Bis(amido) Complex K{Ni[N($SiMe_3$)(2,6-iPr_2-C_6H_3)]$_2$}. *Organometallics* **2014**, *33*, 5566-5570. DOI: 10.1021/om500849u
56. Although new species were observed after heating (50–80 °C) in pentane, the catalytic relevance of the species resulting in noncoordinating solvent were unclear.
57. Performing the analogous experiment with **2** in pentane at room temperature resulted in a color change (mahogany red to yellowed-orange) and afforded a mixture of products detected by ^{1}H NMR. Although recrystallization attempts were unsuccessful, the major components did not exhibit NMR features resembling nickel(I) alkoxides synthesized previously. (Ref 39, 42)
58. Treating the mixed precatalyst system generated in situ with BzN(Boc)$_2$ (**1d**), resulted in burst–lag kinetics with fast consumption of [(SIPr)Ni(C_6D_6)] (within minutes) followed by slow consumption of [Ni(cod)$_2$] and SIPr over the ensuing 24 hours, coupled with line-broadening and presumed decomposition of resulting products (see SI).
59. Haynes, M. T., II; Liu, P.; Baxter, R. D.; Nett, A. J.; Houk, K. N.; Montgomery, J. Dimer Involvement and Origin of Crossover in Nickel-Catalyzed Aldehyde–Alkyne Reductive Couplings. *J. Am. Chem. Soc.* **2014**, *136*, 17495–17504. DOI: 10.1021/ja508909u
60. Zhang, Y.; Wang, Z.; Lamine, W.; Xu, S.; Li, B.; Chrostowska, A.; Miqueu, K.; Liu, S.-Y. Mechanism of Pd/Senphos-Catalyzed trans-Hydroboration of 1,3-Enynes: Experimental and Computational Evidence in Support of the Unusual Outer-Sphere Oxidative Addition Pathway. *J. Org. Chem.* **2023**, *88*, 2415-2424. DOI: 10.1021/acs.joc.2c02841
61. The observation of crossover suggests that C–N oxidative addition is fast and reversible but thermodynamically uphill. As such, the equilibrium concentrations of the resulting nickel(II) acyl species are not detected by NMR or isolable under standard conditions.
62. Yang, L.; Powell, D. R.; Houser, R. P. Structural variation in copper(I) complexes with pyridylmethylamide ligands: structural analysis with a new four-coordinate geometry index, τ_4. *Dalton Trans.* **2007**, 955–964. DOI: 10.1039/B617136B
63. Xie, P.-P.; Qin, Z.-X.; Zhang, S.-Q.; Hong, X. Understanding the Structure-Activity Relationship of Ni-Catalyzed Amide C–N Bond Activation using Distortion/Interaction Analysis. *ChemCatChem* **2021**, *13*, 3536–3542. DOI: 10.1002/cctc.202100672

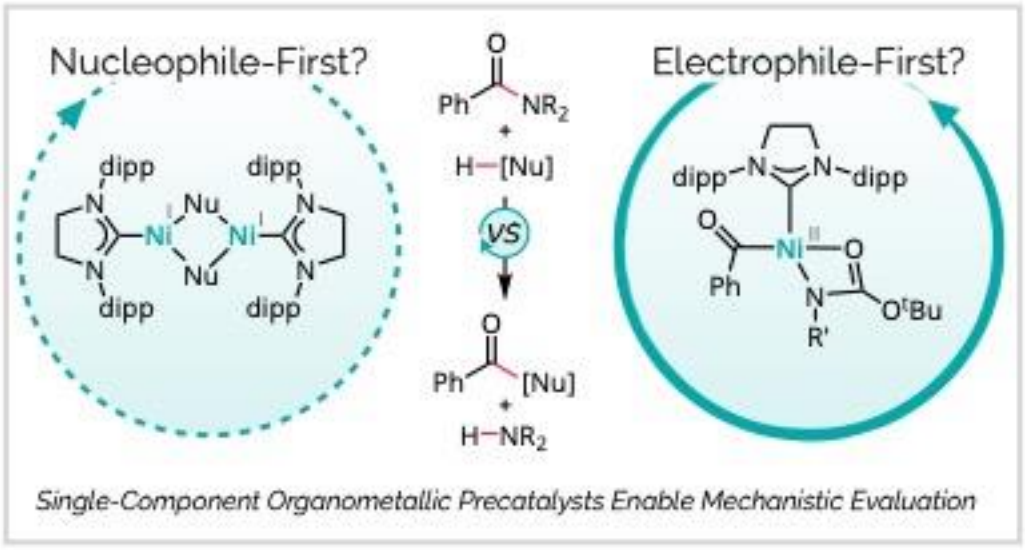

Single-Component Organometallic Precatalysts Enable Mechanistic Evaluation